Exohedrally stabilized C_{70} isomer with adjacent pentagons characterized by crystallography†

Yuan-Zhi Tan, Jia Li, Ming-Yue Du, Shui-Chao Lin, Su-Yuan Xie,* Xin Lu,*
Rong-Bin Huang and Lan-Sun Zheng

All C_{70} isomers other than the well-known D_{5h}-symmetric C_{70} (#8149) are highly elusive due to their defiance of the isolated pentagon rule (IPR), and, in turn, have long been underrated for years. Here we show a non-IPR hollow C_{70} (#8064) with C_2-symmetry stabilized by exohedral chlorination as $^{#8064}C_{70}Cl_{10}$. Its connectivity with two pairs of fused pentagons was determined unambiguously by single crystal X-ray diffraction analysis. Based on the geometric criterion in terms of the pyramidalization angle as well as theoretical computations on the Kekulé structure and the negative nucleus independent chemical shift, the exohedral stabilization of the labile $^{#8064}C_{70}$ is rationalized by releasing the local strain relevant to the fused pentagons and achieving the aromaticity of the remaining sp^2-hybridized carbon framework in the exohedral derivative of $^{#8064}C_{70}$. This new entrant in the C_{70} family, in addition to two previously reported non-IPR isomers (by Yang, Dunsch *et al.* for $Sc_3N@^{#7854}C_{70}$ and by Echegoyen *et al.* for $Sc_2S@^{#7892}C_{70}$), provides valuable opportunities for experimental and theoretical research involving non-IPR isomers of C_{70} beyond the common D_{5h}-C_{70}.

Introduction

C_{70} is one of the prevalent fullerenes having promising properties useful in technological applications. Superior to the most celebrated Buckminsterfullerene, for example, D_{5h}-symmetric C_{70} (#8149, referring to the Fowler–Manolopoulos code[1]) renders broad absorption and excellent photovoltaic performance for fullerene-based organic solar cells.[2,3] In the past quarter century,[4–6] C_{70} research has been overwhelmingly dominated by D_{5h}-symmetric C_{70}. Investigations on other C_{70} isomers have been underrated for years, simply because C_{70} isomers other than D_{5h}-C_{70}, in violation of the isolated pentagon rule (IPR),[7] are highly reactive and practically unavailable in pristine cage form. Both exo- and endohedral derivatizations have been applied to stabilize non-IPR fullerenes. By means of the latter strategy, two non-IPR endohedral C_{70}, *i.e.*, $Sc_3N@^{#7854}C_{70}$ and $Sc_2S@^{#7892}C_{70}$, have recently been isolated by Yang, Dunsch *et al.*[8] and Echegoyen *et al.*[9] However, both of the endofullerenes were assigned by spectrometric methods and computation. Direct determination of the structures of the non-IPR C_{70} isomers by crystallography is still

underway. In this edge article, we report the first hollow non-IPR C_{70} isomer stabilized as chlorofullerene $^{#8064}C_{70}Cl_{10}$ (**1**) by exohedral derivatization. The geometric structure of the C_{70} isomer featuring two pairs of fused pentagons has been identified unambiguously by X-ray crystallography. The possibility of scrutinizing the structure and properties of the hollow non-IPR C_{70} isomer is therefore open.

Results and discussion

Soot containing fullerenes was synthesized in a modified Krätschmer–Huffman arc-discharge reactor[5] under an atmosphere of helium and CCl_4. Extracted using toluene in a supersonic bath, the toluene-soluble components were separated by five stages of HPLC isolation. About 2 mg of the purified $C_{70}Cl_{10}$ was obtained for further identification [the detailed separation procedure is described in the ESI†].

The purified sample was analyzed using an analytical Buckyprep column. As shown in Fig. 1a, the predominant peak at the retention time of ~20.2 min indicates the high purity of the as-purified compound. In the corresponding mass spectrum (Fig. 1b), good agreement of the experimental isotopic pattern of **1** with the simulated one (inset in Fig. 1b) validates the proposed composition of $C_{70}Cl_{10}$. The bare cage of C_{70} (840 m/z) deriving from dechlorination was hardly detected by single-stage mass spectrometry with an atmospheric pressure chemical ionization (APCI) source. Only a minor peak corresponding to a $C_{70}Cl_8$ fragment was recorded even at a furnace temperature of up to 350 °C (Fig. 1b). By contrast, APCI-mass spectra of

State Key Laboratory of Physical Chemistry of Solid Surfaces and Department of Chemistry, College of Chemistry and Chemical Engineering, Xiamen University, Xiamen, 361005, China. E-mail: syxie@xmu.edu.cn; xinlu@xmu.edu.cn; Fax: +86-592-218304; Tel: +86-592-2185191

† Electronic supplementary information (ESI) available: Chromatography, crystallographic information, computational details, and coordinates of optimized pristine $^{#8064}C_{70}$. CCDC 809403. For ESI and crystallographic data in CIF or other electronic format see DOI: 10.1039/c3sc50141h
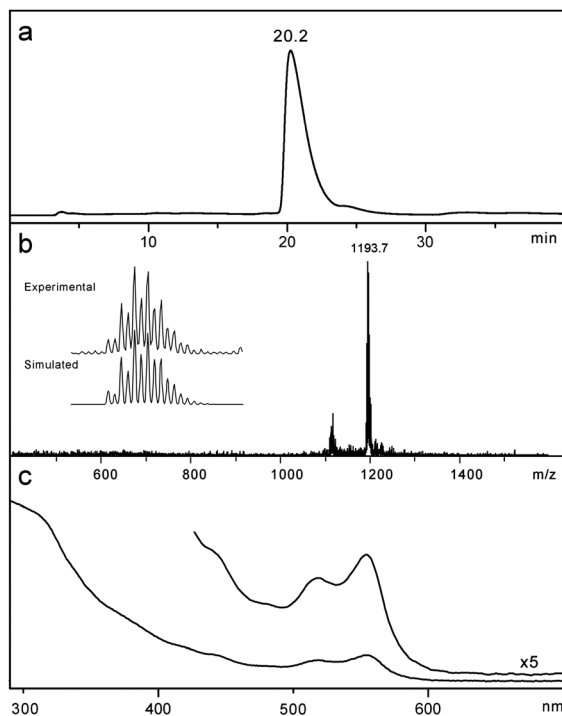
Fig. 1 (a) HPLC chromatogram of purified **1** monitored at 330 nm on an analytical Buckyprep column (I.D. 4.6 × 250 mm) eluting with toluene at a flow rate of 1 ml min⁻¹. (b) Experimental and simulated mass spectra. (c) UV-Vis spectrum of **1** in toluene.

IPR-satisfying D_{5h}-$^{#8149}C_{70}$ chlorides typically contain obvious mass peaks assignable to the pristine fullerene cage of C_{70}.[10–12] The different profiles in the mass spectrometric analyses indicate the thermal stability of **1** superior to the IPR-satisfying chlorofullerenes of D_{5h}-$^{#8149}C_{70}$, as supported by the geometric and theoretical analyses (*vide infra*).

$^{#8064}C_{70}Cl_{10}$ is soluble in common organic solvents, such as toluene, chloroform and carbon disulfide. Its UV/Vis spectrum in toluene shows a broad absorption in the solar spectrum region with visible peaks at 440, 517 and 555 nm. The optical absorption onset of **1** is at ∼600 nm, comparable to the broad absorption of D_{5h}-C_{70} decachloride ($^{#8149}C_{70}Cl_{10}$),[10] with implications for the non-IPR isomer of C_{70} holding attractive potentialities similar to its cousin D_{5h}-C_{70} for promising photovoltaic applications.[2,3]

A single crystal grown from chloroform solution was selected to identify the geometric structure of **1** by X-ray diffraction. The crystallographic data‡ reveal two pairs of fused pentagons on the chiral cage of C_2-symmetric $^{#8064}C_{70}$ (Fig. 2a). The carbon atoms at the pentagon fusions are bonded to four chlorine atoms separately, and the additional six 1,4 positions in the three hexagons are bonded to the remaining six chlorine atoms (Fig. 2a). X-Ray crystallographic data also disclose interesting crystal packing which is relevant to the assembly and charge transport of **1** in the solid state. Three kinds of weak intermolecular interactions (*i.e.*, C–Cl···Cl–C, C–Cl···π and π···π interactions) account for the packing of $^{#8064}C_{70}Cl_{10}$ molecules in the crystal (Fig. 2b). Of interest is the pattern of fullerene molecules in the [101] facets, which is similar to the honeycomb
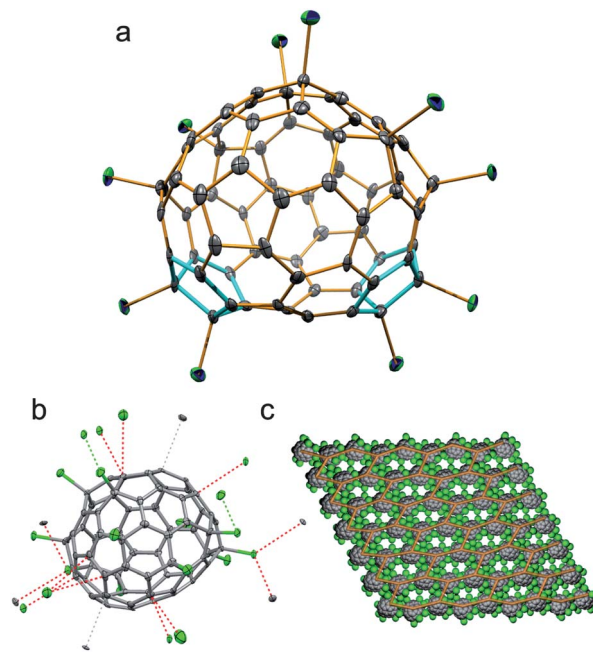
net of graphene (Fig. 2c). Each cavity of this hcb-6³ net is filled by two co-crystallized chloroform molecules, linking to the surrounding $^{#8064}C_{70}Cl_{10}$ molecules through C–Cl···π interactions.

In contrast to the non-IPR C_{70} isomers already-stabilized by encapsulation of endo-clusters (Sc_3N or Sc_2S),[8,9] the exohedral groups of **1** are ready to be removed and sequentially to form a pristine non-IPR C_{70} cage. By stepwise dechlorination through colliding with helium gas in the ion trap of the mass
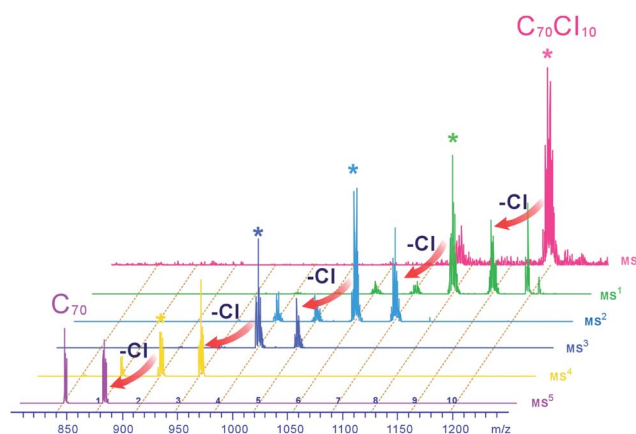

Fig. 2 (a) ORTEP structure of **1** with thermal ellipsoids at 50% probability (the fused pentagons are highlighted in blue). (b) The weak intermolecular interactions involved in the crystal of **1** (the C–Cl···Cl–C, C–Cl···π and π···π interactions are represented as green, red and gray dashed lines, respectively). (c) The hexagonal packing model of [101] facets in the crystal of **1**.

Fig. 3 The stepwise dechlorination of **1**. Multistage mass spectrometry (MS^n, $n =$ 1–5) shows the formation of pristine $^{#8064}C_{70}$ by progressive dechlorination from $^{#8064}C_{70}Cl_m$ ($m =$ 1–10) (m value is indicated as the number in blue on the bottom line, and the species selected for the next stage of the fragmentation are marked with colored asterisks).

spectrometer, as shown in Fig. 3, pristine non-IPR C_2-$^{\#8064}C_{70}$ can be produced from **1** in the gas phase.

To compare the stability of pristine or chlorinated C_{70} isomers, theoretical computations on IPR-satisfying and non-IPR C_{70} species were performed at the GGA-PBE/DNP level of theory.[13,14] As expected, C_2-$^{\#8064}C_{70}$ is less stable than D_{5h}-$^{\#8149}C_{70}$ and is too labile to survive in the ambient conditions. The energy of pristine C_2-$^{\#8064}C_{70}$ is 48.8 kcal mol^{-1} higher than that of D_{5h}-$^{\#8149}C_{70}$, and the HOMO–LUMO gap of non-IPR $^{\#8064}C_{70}$ (0.65 eV) is smaller than that of the IPR one (1.72 eV for D_{5h}-$^{\#8149}C_{70}$). By chlorination, however, the energy of **1** is 10.6 kcal mol^{-1} lower than that of $^{\#8149}C_{70}Cl_{10}$. The band gap of **1** increases to 2.07 eV, close to that of $^{\#8149}C_{70}Cl_{10}$ (2.10 eV).[10] Therefore, in agreement with the mass spectra discussed above, the stability of **1** is higher than the previously synthesized IPR-satisfying $^{\#8149}C_{70}Cl_{10}$.[10] This is also analogous to the cases of previously reported non-IPR chlorofullerenes $^{\#18917}C_{76}Cl_{24}$ (ref. 15) or $^{\#1809}C_{60}Cl_8$ (ref. 16) with lower energies relative to their corresponding IPR-satisfying cousins. Accordingly, it is not surprising that pristine non-IPR $^{\#8064}C_{70}$ is highly elusive but can be captured by chlorination in the solid state. These theoretical data also lend credence to the expectation that numerous isomers of C_{70} with adjacent pentagons might be synthesized and identified in the near future.

With respect to geometric criteria, the local strain of a fullerene molecule can be probed in terms of the pyramidalization angle θ_p.[17] A higher value of θ_p indicates a higher strain of the sp^2-hybridized carbon involved and sequentially facilitates the sp^2-to-sp^3 hybridization conversion. For the pristine $^{\#8064}C_{70}$, the θ_p values of carbon atoms at the pentagon fusions are 16.0 and 14.6°, whereas the other sites have much smaller θ_p values with an average of 10.4° (see the ESI for the coordinates of the computationally optimized $^{\#8064}C_{70}$ in detail†). At the pentagon fusions, therefore, $^{\#8064}C_{70}$ is ready to bond with foreign groups to transfer their hybridization state from sp^2 to sp^3. In addition, the computational electronic structure of pristine $^{\#8064}C_{70}$ shows that larger coefficients of the HOMO and LUMO functions locate at the pentagon fusions, which supports the preferential occurrence of the addition reaction at these sites (see the ESI, Fig. S2†). Indeed, in **1** all the pentagon fusion sites are bonded with chlorine atoms to decrease the θ_p values from ~16.0–14.6° to ~4.0–2.7° (note that the θ_p for an sp^3-hybridized carbon is defined in ref. 18). The strain relief is therefore fulfilled in **1**, similar to the other non-IPR fullerenes stabilized by exohedral derivatization.[15,16,18–28]

The ten sp^3-hybridized carbon atoms in **1** form a ribbon to split the carbon cage of $^{\#8064}C_{70}$ into two sp^2-hybridized C_{30} fragments that are connected by a single C–C bond with a bond length of 1.50 Å (Fig. 4). Based on the criterion of a Kekulé structure, each C_{30} domain contains 38 Kekulé structures.[29] This amount is comparable with those of three previously synthesized polycyclic aromatic hydrocarbon $C_{30}H_{12}$ isomers[30] with 35, 44 and 40 Kekulé structures, respectively (see the ESI, Fig. S3†), suggesting the aromaticity of the resultant sp^2-hybridized carbon fragment in **1**. Among them, 2 Kekulé structures of the C_{30} aromatic fragments are such that no double bonds are located at pentagons, satisfying the so-called
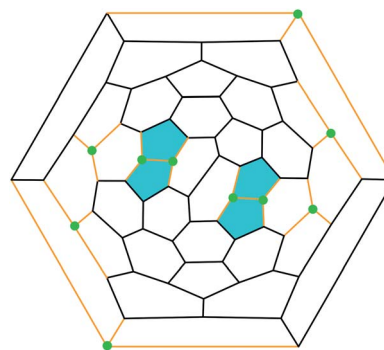

Fig. 4 Schlegel diagram of **1**. The carbon–chlorine atoms are indicated as green dots. The fused pentagons are highlighted in blue. The bonds of the remaining sp^2-hybridized carbon framework are indicated in black.

Taylor criterion.[31] In fact, the crystal data show that all the pentagons of the sp^2-hybridized fragments are composed of single bonds with mean bond lengths of 1.45 Å, whereas the hexagons consist of alternating C=C/C–C bonds ranging from 1.36 to 1.49 Å or approximately equalized bonds ranging from 1.39 to 1.42 Å. Moreover, the aromaticity of the C_{30} fragments is also supported by remarkable negative nucleus independent chemical shift (NICS)[32] values at the centers of rings (see the ESI, Fig. S4 and Table S1†). The local aromaticity in both C_{30} fragments brings additional stability for **1**.[20]

Topologically, the C_2-$^{\#8064}C_{70}$ cage can be transformed to D_{5h}-$^{\#8149}C_{70}$ by two steps of a Stone–Wales (S–W) transformation[33] through a heptagon-incorporating intermediate (Fig. 5). It has been long suspected that fullerene formation may undergo S–W transition.[34] However, the activation barrier for S–W transformation was calculated to be as high as 7–8 eV.[34] Such high barriers imply any S–W transition is hard to fulfil even in temperatures up to a thousand centigrade. In the presence of chlorine, however, conversion of a C_{76} cage from IPR to non-IPR was demonstrated to be viable at a temperature as low as 340 °C.[15] For the present case, the co-existence of the topologically transformable IPR and non-IPR isomers of C_{70} in the chlorine-involving carbon arc-discharge conditions provides a valuable clue to further studies of the S–W mechanism involving C_{70}. However, the possibility and mechanism of such a transformation remains to be detailed in the future.
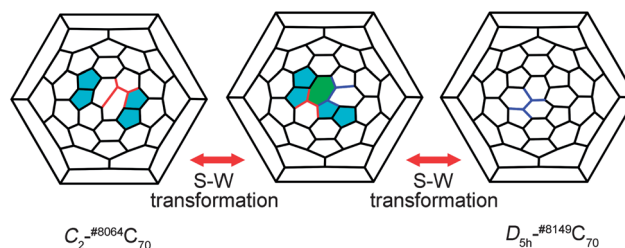

Fig. 5 S–W transformation between C_2-$^{\#8064}C_{70}$ and D_{5h}-$^{\#8149}C_{70}$ through a heptagon-incorporating intermediate. The fused pentagons and heptagon are highlighted in light blue and green, respectively. The C–C bonds involved in the S–W transformation are marked in red or blue.

Conclusions

As a hollow non-IPR member of the C_{70} family, $^{\#8064}C_{70}$ has been stabilized and isolated in the form of $^{\#8064}C_{70}Cl_{10}$. Its geometric structure, with two pairs of fused pentagons in an inherent chiral C_2-symmeric cage, was unambiguously characterized by X-ray crystallography. Computational and geometrical analyses disclose the stabilization effects of $^{\#8064}C_{70}Cl_{10}$ in terms of strain relief and local aromaticity.[20] The newly identified $^{\#8064}C_{70}Cl_{10}$ exemplifies higher stability of the non-IPR C_{70} chloride, new insight into the C_{70} formation mechanism, as well as potentially useful properties of non-IPR C_{70} species with broad absorption. Starting from this work, we expected that further investigations of macroscopic synthesis, the formation mechanism and promising applications of C_{70} isomers with adjacent pentagon configurations might be stimulated.

Acknowledgements

Notes and references

‡ Crystal of $C_{70}Cl_{10}$: $0.15 \times 0.12 \times 0.02$ mm; triclinic; space group $P\bar{1}$; $a = 11.049(3)$, $b = 13.430(4)$, $c = 18.364(5)$ Å; $\alpha = 105.567(4)$, $\beta = 91.091(4)$, $\gamma = 106.254(4)°$; $V = 2507.1(11)$ Å^3; $Z = 2$; $T = 173(2)$ K; no. reflections = 17 260; no. independent reflections = 8382; full-matrix least-squares refinement on F^2; final R indices ($F_o > 4\sigma(F_o)$) are $R_1 = 0.0867$ and w$R_2 = 0.2162$ (R_1(all data) = 0.1057 and wR_2(all data) = 0.2342).

1 P. W. Fowler and D. E. Manolopoulos, *An Atlas of Fullerenes*, Oxford University Press, Oxford, 1995.

2 B. C. Thompson and J. M. J. Frechet, *Angew. Chem., Int. Ed.*, 2008, **47**, 58–77.

3 Y. He and Y. Li, *Phys. Chem. Chem. Phys.*, 2011, **13**, 1970–1983.

4 H. W. Kroto, J. R. Heath, S. C. O'Brien, R. F. Curl and R. E. Smalley, *Nature*, 1985, **318**, 162–163.

5 W. Kratschmer, L. D. Lamb, K. Fostiropoulos and D. R. Huffman, *Nature*, 1990, **347**, 354–358.

6 A. Hirsch and M. Brettreich, *Fullerenes: Chemistry and Reactions*, Wiley-VCH Verlag GmbH & Co. KGaA, London, 2005.

7 H. W. Kroto, *Nature*, 1986, **329**, 529–531.

8 S. F. Yang, A. A. Popov and L. Dunsch, *Angew. Chem., Int. Ed.*, 2007, **46**, 1256–1259.

9 N. Chen, M. Mulet-Gas, Y.-Y. Li, R. E. Stene, C. W. Atherton, A. Rodriguez-Fortea, J. M. Poblet and L. Echegoyen, *Chem. Sci.*, 2013, **4**, 180–186.

10 P. R. Birkett, A. G. Avent, A. D. Darwish, H. W. Kroto, R. Taylor and D. R. M. Walton, *J. Chem. Soc., Chem. Commun.*, 1995, 683–684.

11 I. V. Kuvychko, A. V. Streletskii, N. B. Shustova, K. Seppelt, T. Drewello, A. A. Popov, S. H. Strauss and O. V. Boltalina, *J. Am. Chem. Soc.*, 2010, **132**, 6443–6462.

12 I. V. Kuvychko, A. A. Popov, A. V. Streletskii, L. C. Nye, T. Drewello, S. H. Strauss and O. V. Boltalina, *Chem. Commun.*, 2010, **46**, 8204–8206.

13 B. Delley, *J. Chem. Phys.*, 1990, **92**, 508–517.

14 B. Delley, *J. Chem. Phys.*, 2000, **113**, 7756–7764.

15 I. N. Ioffe, A. A. Goryunkov, N. B. Tamm, L. N. Sidorov, E. Kemnitz and S. I. Troyanov, *Angew. Chem., Int. Ed.*, 2009, **48**, 5904–5907.

16 Y. Z. Tan, Z. J. Liao, Z. Z. Qian, R. T. Chen, X. Wu, H. Liang, X. Han, F. Zhu, S. J. Zhou, Z. P. Zheng, X. Lu, S. Y. Xie, R. B. Huang and L. S. Zheng, *Nat. Mater.*, 2008, **7**, 790–794.

17 R. C. Haddon, *Science*, 1993, **261**, 1545–1550.

18 X. Han, S. J. Zhou, Y. Z. Tan, X. Wu, F. Gao, Z. J. Liao, R. B. Huang, Y. Q. Feng, X. Lu, S. Y. Xie and L. S. Zheng, *Angew. Chem., Int. Ed.*, 2008, **47**, 5340–5343.

19 C. R. Wang, Z. Q. Shi, L. J. Wan, X. Lu, L. Dunsch, C. Y. Shu, Y. L. Tang and H. Shinohara, *J. Am. Chem. Soc.*, 2006, **128**, 6605–6610.

20 Y. Z. Tan, S. Y. Xie, R. B. Huang and L. S. Zheng, *Nat. Chem.*, 2009, **1**, 450–460.

21 K. Ziegler, A. Mueller, K. Y. Amsharov and M. Jansen, *J. Am. Chem. Soc.*, 2010, **132**, 17099–17101.

22 Y. Z. Tan, T. Zhou, J. Bao, G. J. Shan, S. Y. Xie, R. B. Huang and L. S. Zheng, *J. Am. Chem. Soc.*, 2010, **132**, 17102–17104.

23 Y. Z. Tan, J. Li, T. Zhou, Y. Q. Feng, S. C. Lin, X. Lu, Z. P. Zhan, S. Y. Xie, R. B. Huang and L. S. Zheng, *J. Am. Chem. Soc.*, 2010, **132**, 12648–12652.

24 Y. Z. Tan, J. Li, F. Zhu, X. Han, W. S. Jiang, R. B. Huang, Z. Zheng, Z. Z. Qian, R. T. Chen, Z. J. Liao, S. Y. Xie, X. Lu and L. S. Zheng, *Nat. Chem.*, 2010, **2**, 269–273.

25 Y. Z. Tan, R. T. Chen, Z. J. Liao, J. Li, F. Zhu, X. Lu, S. Y. Xie, J. Li, R. B. Huang and L. S. Zheng, *Nat. Commun.*, 2011, **2**, 1431–1436.

26 K. Ziegler, A. Mueller, K. Y. Amsharov and M. Jansen, *Chem.–Asian J.*, 2011, **6**, 2412–2418.

27 T. Zhou, Y. Z. Tan, G. J. Shan, X. M. Zou, C. L. Gao, X. Li, K. Li, L. L. Deng, R. B. Huang, L. S. Zheng and S. Y. Xie, *Chem.–Eur. J.*, 2011, **17**, 8529–8532.

28 K. Y. Amsharov, K. Ziegler, A. Mueller and M. Jansen, *Chem.–Eur. J.*, 2012, **18**, 9289–9293.

29 D. J. Klein and X. Liu, *J. Comput. Chem.*, 1991, **12**, 1260.

30 S. Hagen, M. S. Bratcher, M. S. Erickson, G. Zimmermann and L. T. Scott, *Angew. Chem., Int. Ed. Engl.*, 1997, **36**, 406–408.

31 R. Taylor, *J. Chem. Soc., Perkin Trans. 2*, 1992, 3.

32 P. v. R. Schleyer, C. Maerker, A. Dransfeld, H. Jiao and N. J. R. v. E. Hommes, *J. Am. Chem. Soc.*, 1996, **118**, 6317–6318.

33 A. J. Stone and D. J. Wales, *Chem. Phys. Lett.*, 1986, **128**, 501–503.

34 H. F. Bettinger, B. I. Yakobson and G. E. Scuseria, *J. Am. Chem. Soc.*, 2003, **125**, 5572–5580.